ACS Sustainable Chemistry & Engineering

Research Article

pubs.acs.org/journal/ascecg

Ionic Liquid-Assisted Synthesis of Au−Pt Bimetallic Particles for Enhanced Methanol Electrooxidation

Zhonghao Li*,† and Qian Niu‡

†Key Laboratory of Colloid and Interface Chemistry, Shandong University, Ministry of Education, Jinan, 250100, China
‡School of Materials Science and Engineering, Shandong University, Jinan, 250061, China

ABSTRACT: A facile ionic liquid-assisted route is proposed for the successful synthesis of Au−Pt bimetallic particles with a core−shell structure at room temperature. The synthesized bimetallic particles exhibit flowerlike morphologies with a tunable composition (Au and Pt) by controlling the molar ratios between metal precursors. Specifically, the synthesized Au−Pt particles exhibit efficient electrocatalytic activities toward methanol oxidation in alkaline media, which indicates their useful application in direct methanol fuel cells.

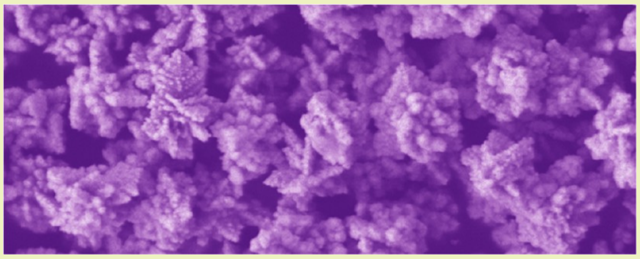

KEYWORDS: *Ionic liquid, Bimetallic particles, Nanostructures, Electroactivity*

■ INTRODUCTION

Ionic liquids (ILs) are probably among the most actively researched compounds of the recent past.[1] Recently, ILs have received increasing attention from the inorganic materials community because synthesis in ILs occasionally results in materials that are difficult or impossible to obtain by using other synthesis routes. Various inorganic nanomaterials with controlled structures and improved properties have already been reported in ILs.[2−15] However, most of the researches are on the synthesis of single component inorganic materials in ILs.[16−18] Therefore, it is of great interest to explore the flexibility of ILs for the synthesis of multicomponent inorganic materials.

Recently, bimetallic particles have been attracting great interest because the shape, size, and composition of bimetallic nanostructures significantly influence their catalytic properties.[19] Specifically, interesting electrochemical behavior is exhibited by the synergistic effect of the elements from the bimetallic particles, which usually makes them better catalysts than the pure metals alone.[20,21] Presently, the synthesis of monometallic particles based on IL routes have already demonstrated its bright future.[18] However, the number of publications on bimetallic particles based on IL routes is comparatively low, which are mainly limited in the electrodeposition[22] or sputter deposition technique.[23] Besides these methods, we have recently shown that the Au−Pd bimetallic particles can be synthesized by an IL-assisted route,[24] which indicates it might be a promising method for fabrication of bimetallic particles.

The synthesis and electrochemical application of Pt-based nanocatalyst is very important due to its potential applications in the electrochemical energy conversion and storage.[25−27] Herein, we report on the synthesis of Au−Pt bimetallic particles with the assistance of the ionic liquid 1-butyl-3-methyl imidazolium bromide ([BMIM]Br) at room temperature. Specifically, the flowerlike Au−Pt bimetallic particles with core−shell structures can be synthesized by the present route. In particular, the synthesized Au−Pt particles exhibit efficient electrocatalytic activities toward methanol oxidation in alkaline media, which indicates their useful application in direct methanol fuel cells.

■ EXPERIMENTAL SECTION

Synthesis. In a typical synthesis of Au_1Pt_3 particles, an aqueous solution of $HAuCl_4·4H_2O/H_2PtCl_6·5H_2O$ mixture in a molar ratio of 1:3 (2 mL, 5 mM) was first prepared. Then, 1-butyl-3-methyl imidazolium bromide ([BMIM]Br) was added into the above solution to result in 5 mM [BMIM]Br. Then, an aqueous solution of L-ascorbic acid (0.1 mL, 1 M) was injected with gentle shaking. After this, the solution was kept at room temperature for 20 h. Finally, the products were centrifuged and washed with water and ethanol several times. The procedure for synthesis of particles with other molar ratios ($HAuCl_4·4H_2O/H_2PtCl_6·5H_2$Ò 0:1, 1:1, 3:1, and 1:0) is similar to the above description. The synthesis with sodium bis(2-ethylhexyl) sulfosuccinate (AOT) is similar to above description.

Characterization. X-ray diffraction was performed using a Rigaku Dmax-rc X-ray diffractometer. SEM was performed using a Hitachi SU-70 FESEM. HAADF-STEM and HAADF-STEM-EDS mapping characterizations were performed using a JEM-2100F. The compositions of the bimetallic particles were determined by inductively coupled plasma atomic emission spectroscopy (ICP-AES).

Electrocatalytic Activities. Electrochemical measurements were performed with a conventional three electrode test cell containing a glassy carbon electrode (GCE) (diameter: 3 mm) as working electrode, Pt foil electrode as counter electrode, and saturated calomel electrode (SCE) as reference electrode. To modify GCE, 6 μL of aqueous particle solution (2 mg mL^{-1}) of Pt, Au, or Au−Pt particles was dropped onto the surface of the GCE. After the solution was

Received: November 11, 2013
Revised: December 2, 2013
Published: December 10, 2013

dried, 5 μL of Nafion solution (0.05% wt) was added. The dried GCE was cleaned again by sequentially washing with ethanol and water. For methanol oxidation, the CVs were measured in 0.5 M KOH solution and 0.5 M KOH + 0.5 M methanol solution at a scan rate of 50 mV s^{-1}. The chronoamperometry of the catalysts was tested, respectively. The electrolyte solutions were purged with high purity N_2 gas for 20 min before use.

■ RESULTS AND DISCUSSION

Figure 1a shows the XRD patterns of the as-prepared Au_1Pt_3 bimetallic particles. The XRD pattern of the Au_1Pt_3 bimetallic particles shows both Au fcc and Pt fcc peaks, indicating the formation of a non-alloyed state. Figure 1b and c show typical low and high magnification SEM images, respectively, of the synthesized Au_1Pt_3 sample (the feeding molar ratio of $HAuCl_4\cdot 4H_2O$ to $H_2PtCl_6\cdot 5H_2O$ is 1:3), manifesting the formation of flowerlike particles with the size of 923 ± 88 nm. The ICP-AES analysis indicates the atomic ratios of Au and Pt are in agreement with the feed ratio of metal salts (Au_1Pt_3), representing the complete reduction of the reaction. The elemental mapping of Au and Pt shown in Figure 1e−g obtained by high-angle annular dark-field scanning TEM and energy-dispersive X-ray spectroscopy (HAADF-STEM-EDS) indicates that Au is mainly distributed in the core of the particle, while Pt is mainly distributed at the outer edge of the flowerlike particles. This clearly indicates that the synthesized flowerlike Au−Pt particles are in a core−shell structure. The formation of the Au−Pt core−shell particles can be attributed to the difference in the standard reduction potentials of the Au(III) and Pt(IV) species. Because of the large difference in the reduction potential of Au^{3+} ($AuCl_4^-$/Au, +1.002 V vs SHE) and Pt^{4+} ($PtCl_6^{2-}$/Pt, +0.742 V vs SHE), the reduction of Au ions preferentially occurs first to produce Au cores, which is followed by overgrowth of the Pt particles on the Au seeds with the assistance of an ionic liquid. It is well known that the ionic liquid could be selectively adsorbed on the inorganic crystal surfaces.[8] Such selective adsorption can alter the anisotropic growth process and produce well-defined morphologies. This can explain the flowerlike particles formed with the assistance of [BMIM]Br.

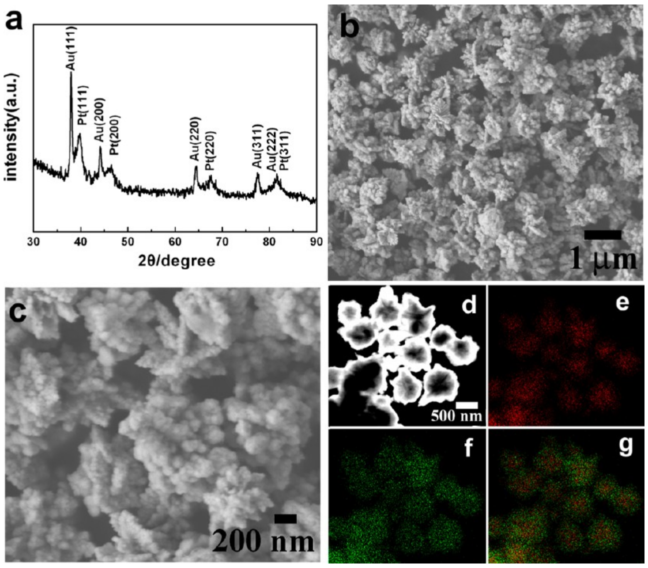

Figure 1. (a) XRD pattern, (b, c) low and high magnification SEM images of as-prepared Au_1Pt_3 bimetallic particles recovered at 5 mM [BMIM]Br, respectively, (d) HAADF-STEM image, and (e−g) EDS mapping images of Au_1Pt_3 bimetallic particles (e, Au with red color; f, Pt with green color; and g, overlap image of Au and Pt).

In order to understand whether the present [BMIM]Br ionic liquid plays a key role for the formation of flowerlike particles, the controlled synthesis without the assistance of [BMIM]Br is performed with the synthesis condition similar to that of Figure 1. Figure 2a shows the SEM image of the Au_1Pt_3 sample obtained without [BMIM]Br. It is found that spherical particles with the size of 68 ± 19 nm form. Furthermore, to understand whether the role of the present ionic liquid is similar to that of the common surfactant, we also synthesize the particles with the assistance of a common surfactant. Here, the sodium bis(2-ethylhexyl) sulfosuccinate (AOT) is chosen as the studied surfactant because it has been widely used in the synthesis of inorganic particles. Figure 2b shows SEM image of the Au_1Pt_3 sample obtained with 5 mM AOT. It is found that the product is also in spherical morphology with the size of 105 ± 21 nm. Therefore, it is clear that the [BMIM]Br plays an important role for the formation of the as-prepared flowerlike particles. Figure 2c shows the SEM image of the product recovered at 50 mM [BMIM]Br. It is found that the product is not as well-defined as the flowerlike particles that are recovered at 5 mM [BMIM]Br (Figure 1). This indicates that the concentration of [BMIM]Br also has an important influence on the synthesized particles.

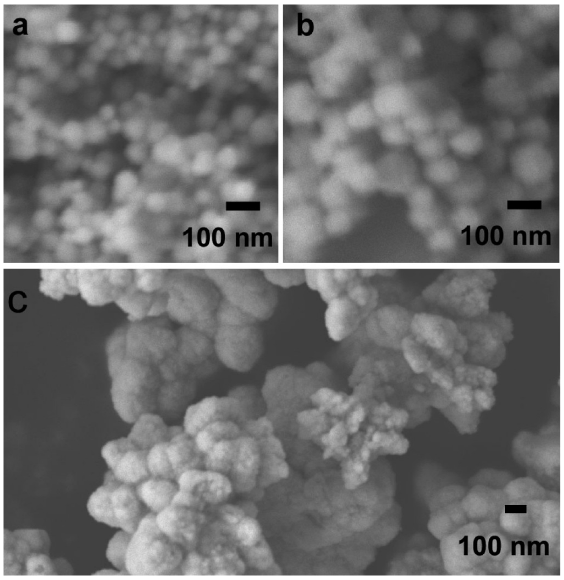

Figure 2. SEM images of the Au_1Pt_3 bimetallic particles synthesized without [BMIM]Br (a), with 5 mM AOT (b), and with 50 mM [BMIM]Br (c).

To understand whether the Au−Pt bimetallic particles with controlled composition could be obtained by the present synthetic route, we perform synthesis experiments at various molar ratios of $HAuCl_4\cdot 4H_2O$ and $H_2PtCl_6\cdot 5H_2O$ (0:1 as Pt, 1:1 as Au_1Pt_1, 3:1 as Au_3Pt_1, and 1:0 as Au). Figure 3a shows SEM images of samples obtained at various metal precursor molar ratios. For the pure Pt, it is found that irregular aggregates form with the size of 430 ± 96 nm for the larger aggregates. For Au_1Pt_1 and Au_3Pt_1, the synthesized particles have a flowerlike morphology (Figure 3b and c), which is similar to the Au_1Pt_3 product in Figure 1. The size of the particles is 601 ± 91 and 424 ± 102 nm, respectively, for

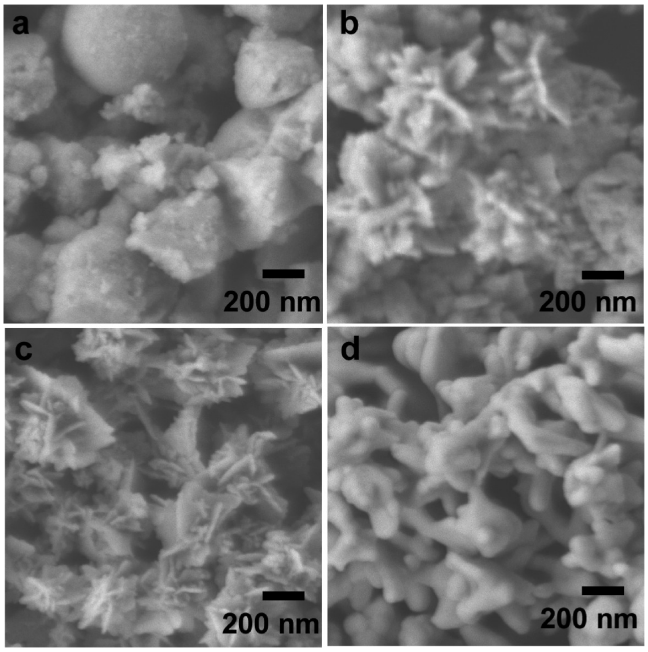

Figure 3. SEM images of the synthesized various Au−Pt bimetallic particles with controlled compositions recovered at 5 mM [BMIM]Br: (a) Pt, (b) Au_1Pt_1, (c) Au_3Pt_1, and (d) Au.

Au_1Pt_1, and Au_3Pt_1. The ICP-AES analysis indicates the atomic ratios of Au and Pt are in agreement with the feed ratio of metal salts (Au_1Pt_1 and Au_3Pt_1). When the reaction is performed with the single component $HAuCl_4 \cdot 4H_2O$, it is found that irregular gold aggregates form with the size of 352 ± 73 nm. Summarizing the above results, therefore, the composition of the Au−Pt bimetallic particles synthesized by the present ionic liquid route could be well controlled.

To evaluate the electrocatalytic activities of the synthesized Au−Pt bimetallic particles, the electrocatalytic properties toward methanol oxidation are tested due to its important application in direct methanol fuel cells. Figure 4a shows the cyclic voltammograms (CVs) of the various catalysts in a 0.5 M KOH aqueous solution. The calculated electrochemically active surface areas (ECSA) are 1.26, 1.39, 1.28, 1.12, and 0.24 $m^2\ g^{-1}$ for Pt, Au_1Pt_3, Au_1Pt_1, Au_3Pt_1, and Au particles, respectively. Figure 4b shows the ECSA-normalized CVs of methanol oxidation with the various catalysts in a 0.5 M KOH solution containing 0.5 M methanol. Characteristic anodic peaks in the forward and reverse sweeps associated with methanol oxidation are observed. The ECSA-normalized peak current densities are 1.93, 9.56, 7.28, 5.98, and 0.17 mA cm^{-2} for the Pt, Au_1Pt_3, Au_1Pt_1, Au_3Pt_1, and Au particles, respectively (Figure 4c). It is clear that the Au−Pt bimetallic particles have superior catalytic properties than those of the synthesized Au and Pt catalyst. Because the current densities are normalized to the ECSA, the superior catalytic properties of the Au−Pt bimetallic particles could be ascribed to the synergistic catalytic effect from the bimetals. Among the studied Au−Pt bimetallic particles, it is found that Au_1Pt_3 shows much higher activity for the oxidation of methanol. In particular, the corresponding mass activity (133.5 mA mg^{-1}, Figure 4c) of the Au_1Pt_3 particles is about 3.2 times higher than the reported commercial Pt/C catalysts (41.1 mA mg^{-1}).[28] The electrochemical stability of the Au−Pt bimetallic catalysts for methanol oxidation is also investigated by chronoamperometry (CA) experiments (Figure 4d). It is shown that the current decay of Au_1Pt_3 bimetallic particles is slower than that of the others, which indicates their better electrochemical stability and electrocatalytic activity. The differences in electrocatalytic activity of the various Au−Pt bimetallic particles may be attributed to their different compositions and surface structures. As discussed above, the obtained Au_1Pt_3 particles show enhanced catalytic properties, which demonstrate their promising application in fuel cells.

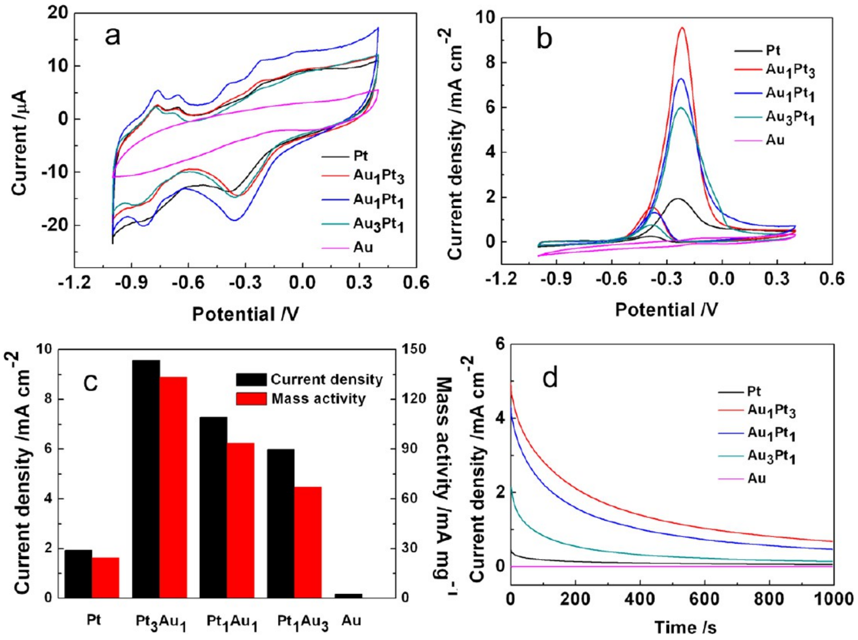

Figure 4. CVs of various catalysts in (a) 0.5 M KOH. (b) ECSA-normalized CVs of various catalysts in 0.5 M KOH + 0.5 M methanol, scan rate: 50 mV/s. (c) ECSA-normalized current densities and mass activities for methanol oxidation. (d) Chronoamperometric curves of catalysts in 0.5 M KOH + 0.5 M methanol at −0.2 V.

CONCLUSIONS

In summary, we suggest a facile ionic liquid-assisted route for the synthesis of composition-controllable flowerlike Au−Pt bimetallic particles with core−shell structure at room temperature. By comparison with the controlled experiments, it is found that the ionic liquid plays an important role in the formation of these interesting flowerlike particles. The studies of electrocatalytic activities demonstrate that the as-prepared Au_1Pt_3 bimetallic particles have remarkably enhanced electrocatalytic properties toward methanol oxidation compared with pure Au, pure Pt, and reported commercial Pt/C catalysts, indicating their useful applications in fuel cells. Moreover, this work provides a promising synthesis strategy for developing efficient catalysts of fuel cells, which might be applicable to other multicomponent metal particles with enhanced electroactivities.

AUTHOR INFORMATION

Corresponding Author

*Fax: (+86) 531-88564750. E-mail: zhonghaoli@sdu.edu.cn.

Notes

The authors declare no competing financial interest.

ACKNOWLEDGMENTS

This work is supported by National Natural Science Foundation of China (NSFC, No. 21173127).

REFERENCES

(1) Taubert, A.; Stange, F.; Li, Z.; Junginger, M.; Gunter, C.; Neumann, M.; Friedrich, A. CuO nanoparticles from the strongly hydrated ionic liquid precursor (ILP) tetrabutylammonium hydroxide: Evaluation of the ethanol sensing activity. *ACS Appl. Mater. Interfaces* **2012**, *4*, 791−795.

(2) Wang, Y.; Yang, H. Synthesis of CoPt nanorods in ionic liquids. *J. Am. Chem. Soc.* **2005**, *127*, 5316−5317.

(3) Ding, K.; Miao, Z.; Liu, Z.; Zhang, Z.; Han, B.; An, G.; Miao, S.; Xie, Y. Synthesis of high quality TiO_2 nanocrystals in ionic liquid via a microwave-assisted process. *J. Am. Chem. Soc.* **2007**, *129*, 6362−6363.

(4) Parnham, E. R.; Morris, R. E. Facile ionothermal synthesis of zeolites, metal−organic frameworks, and inorganic−organic hybrids. *Acc. Chem. Res.* **2007**, *40*, 1005−1013.

(5) Kaper, H.; Endres, F.; Djerdj, I.; Antonietti, M.; Smarsly, B.; Maier, J.; Hu, Y. S. Direct low-temperature synthesis of rutile nanostructures in ionic liquids. *Small* **2007**, *3*, 1753−1763.

(6) Delahaye, E.; Xie, Z. L.; Schaefer, A.; Douce, L.; Rogez, G.; Rabu, P.; Gunter, C.; Gutmann, J. S.; Taubert, A. Intercalation synthesis of functional hybrid materials based on layered simple hydroxide hosts and ionic liquid guests − a pathway towards multifunctional ionogels without a silica matrix. *Dalton Trans.* **2011**, *40*, 9977−9988.

(7) Wender, H.; Migowski, P.; Feil, A. F.; de Oliveira, L. F.; Prechtl, M. H. G.; Giovanna Machado, R.; Teixeira, S. R.; Dupont, J. On the formation of anisotropic gold nanoparticles by sputtering onto a nitrile functionalised ionic liquid. *Phys. Chem. Chem. Phys.* **2011**, *13*, 13552−13557.

(8) Lian, J.; Duan, X.; Ma, J.; Peng, P.; Kim, T.; Zheng, W. J. Hematite (alpha-Fe_2O_3) with various morphologies: Ionic liquid-assisted synthesis, formation mechanism, and properties. *ACS Nano* **2009**, *3*, 3749−3761.

(9) Richter, K.; Birkner, A.; Mudring, A. V. Stabilizer-free metal nanoparticles and metal−metal oxide nanocomposites with long-term stability prepared by physical vapor deposition into ionic liquids. *Angew. Chem., Int. Ed.* **2010**, *49*, 2431−2435.

(10) Hoang, P.; Park, H.; Kim, D. Ultrafast and continuous synthesis of unaccommodating inorganic nanomaterials in droplet- and ionic liquid-assisted microfluidic system. *J. Am. Chem. Soc.* **2011**, *133*, 14765−14770.

(11) Zhao, Y. J.; Zhang, J. L.; Han, B. X.; Song, J. L.; Li, J. S.; Wang, Q. A. Metal-organic framework nanospheres with well-ordered mesopores synthesized in an ionic liquid/CO_2/surfactant system. *Angew. Chem., Int. Ed.* **2011**, *50*, 636−639.

(12) Xiao, L.; Shen, H.; von Hagen, R.; Pan, J.; Lhoussaine, B.; Mathur, S. Microwave assisted fast and facile synthesis of SnO_2 quantum dots and their printing applications. *Chem. Commun.* **2010**, *46*, 6509−6511.

(13) Zein El Abedin, S .; Endres, F. Electrodeposition of metals and semiconductors in air- and water-stable ionic liquids. *ChemPhysChem* **2006**, *7*, 58−61.

(14) Freudenmann, D.; Wolf, S.; Wolff, M.; Feldmann, C. Ionic liquids: New perspectives for inorganic synthesis. *Angew. Chem., Int. Ed.* **2011**, *50*, 11050−11060.

(15) Yang, J. M.; Gou, S. P.; Sun, I. W. Single-step large-scale and template-free electrochemical growth of Ni−Zn alloy filament arrays from a zinc chloride based ionic liquid. *Chem. Commun.* **2010**, *46*, 2686−2688.

(16) Antonietti, M.; Kuang, D.; Smarsly, B.; Zhou, Y. Ionic liquids for the convenient synthesis of functional nanoparticles and other inorganic nanostructures. *Angew. Chem., Int. Ed.* **2004**, *43*, 4988−4992.

(17) Taubert, A.; Li, Z. Inorganic materials from ionic liquids. *Dalton Trans.* **2007**, *7*, 723−727.

(18) Ma, Z.; Yu, J. H.; Dai, S. Preparation of inorganic materials using ionic liquids. *Adv. Mater.* **2010**, *22*, 261−285.

(19) Lee, Y. W.; Kim, M. J.; Kim, Z. H.; Han, S. W. One-step synthesis of Au@Pd core-shell nanooctahedron. *J. Am. Chem. Soc.* **2009**, *131*, 17036−17037.

(20) Zhai, Y.; Zhai, J.; Dong, S. Temperature-dependent synthesis of CoPt hollow nanoparticles: From "nanochain" to "nanoring. *Chem. Commun.* **2010**, *46*, 1500−1502.

(21) Ataee-Esfahani, H.; Wang, L.; Nemoto, Y.; Yamauchi, Y. Synthesis of bimetallic Au@Pt nanoparticles with Au core and nanostructured Pt shell toward highly active electrocatalysts. *Chem. Mater.* **2010**, *22*, 6310−6318.

(22) Endres, F.; Bukowski, M.; Hempelmann, R.; Natter, H. Electrodeposition of nanocrystalline metals and alloys from ionic liquids. *Angew. Chem., Int. Ed.* **2003**, *42*, 3428−3430.

(23) Suzuki, S.; Suzuki, T.; Tomita, Y.; Hirano, M.; Okazaki, K.; Kuwabata, S.; Torimoto, T. Compositional control of AuPt nanoparticles synthesized in ionic liquids by the sputter deposition technique. *CrystEngComm* **2012**, *14*, 4922−4926.

(24) Li, Z.; Li, R.; Mu, T.; Luan, Y. Ionic liquid assisted synthesis of Au−Pd bimetallic particles with enhanced electrocatalytic activity. *Chem.—Eur. J.* **2013**, *19*, 6005−6013.

(25) Wang, L.; Yamauchi, Y. Metallic nanocages: Synthesis of bimetallic Pt−Pd hollow nanoparticles with dendritic shells by selective chemical etching. *J. Am. Chem. Soc.* **2013**, *135*, 16762−16765.

(26) Dong, S.; Chen, X.; Wang, S.; Gu, L.; Zhang, L.; Wang, X.; Zhou, X.; Liu, Z.; Han, P.; Duan, Y.; Xu, H.; Yao, J.; Zhang, C.; Zhang, K.; Cui, G.; Chen, L. 1D coaxial platinum/titanium nitride nanotube arrays with enhanced electrocatalytic activity for the oxygen reduction reaction: towards Li−air batteries. *ChemSusChem* **2012**, *5*, 1712−1715.

(27) Xia, B.; Wu, H.; Yan, Y.; Lou, X.; Wang, X. Ultrathin and ultralong single-crystal platinum nanowire assemblies with highly stable electrocatalytic activity. *J. Am. Chem. Soc.* **2013**, *135*, 9480−9485.

(28) Kuai, L.; Wang, S.; Geng, B. Gold−platinum yolk−shell structure: A facile galvanic displacement synthesis and highly active electrocatalytic properties for methanol oxidation with super CO-tolerance. *Chem. Commun.* **2011**, *47*, 6093−6095.